Kybernetika

Ronghua Lei; Li Chen

Observer-based adaptive sliding mode fault-tolerant control for the underactuated space robot with joint actuator gain faults

Kybernetika, Vol. 57 (2021), No. 1, 160–173

Persistent URL: http://dml.cz/dmlcz/149032

KYBERNETIKA — VOLUME 57 (2021), NUMBER 1, PAGES 160–173

OBSERVER-BASED ADAPTIVE SLIDING MODE FAULT-TOLERANT CONTROL FOR THE UNDERACTUATED SPACE ROBOT WITH JOINT ACTUATOR GAIN FAULTS

Ronghua Lei and Li Chen

An adaptive sliding mode fault-tolerant controller based on fault observer is proposed for the space robots with joint actuator gain faults. Firstly, the dynamic model of the underactuated space robot is deduced combining conservation law of linear momentum with Lagrange method. Then, the dynamic model of the manipulator joints is obtained by using the mathematical operation of the block matrices, hence the measurement of the angular acceleration of the base attitude can be omitted. Subsequently, a fault observer which can accurately estimate the gain faults is designed, and the estimated results are fed back to the adaptive sliding mode fault-tolerant controller. It is proved that the proposed control algorithm can guarantee the global asymptotic stability of the closed-loop system through the Lyapunov theorem. The simulation results authenticate the effectiveness and feasibility of the control strategy and observation scheme.

Keywords: space robot, underactuated, actuator gain fault, fault observer, fault-tolerant

Classification: 93C10, 03C65, 34D20

1. INTRODUCTION

Different from the industrial robot whose base is fixed, the base of the space robot is in free-floating state, so the degrees of freedom of the latter is more than those of the former, and there is dynamic coupling and kinematic coupling between the base and the manipulators [2, 17, 28]. The position and attitude of the base of space robot are adjusted by a momentum flywheel or a jet thruster, while the rotations of the manipulators are controlled by joint motors, i. e., actuators. Considering the high cost of the jet fuel in space, the position and attitude of the base are usually not controlled. Thus, the space robot is a kind of nonlinear underactuated system. The space robot can assist astronaut to complete a series of high-risk space tasks, such as spacecraft on-orbit assembly, satellite maintenance and visual inspection [3, 13, 15, 27], so it can improve the efficiency of space exploration and reduce the cost. The dynamics and control of the space robots have attracted great attention of the space technicians all over the world. At present, the space robots are usually regarded as a class of multi-rigid-body systems,

DOI: 10.14736/kyb-2021-1-0160

and various modeling methods are proposed to describe its kinematic or dynamic characteristics by relevant scholars. Combining Lagrange method and conservation law of linear momentum, Evangelos [14, 16] deduced the explicit dynamic model of the space robot, which can fully reflect the dynamic characteristics of the system. Considering the linear momentum conservation as the constraint of the system, Vafa et al. [24, 25] put forward the concept of virtual manipulator (VM), which can be used for the kinematic modeling, workspace analysis and inverse kinematics solution, and kinematic model can also effectively reduce the interference of the base on the trajectory plannings of the manipulators. Based on the principle of generalized inertia tensor (GIT) of the ground fixed-base manipulators, Yoshida [22, 23] proposed the concept of extended generalized inertia tensor (EGIT), which can be used to calculate the contact force between the end gripper of the space robot and the target. More recently, He [7, 6] established the PDE model for the flexible robotic manipulator with input backlash, and proposed a adaptive fuzzy control strategy for an uncertain constrained robot using impedance learning method, which can provide new ideas for the modeling and control scheme design of the space robot.

The high-speed rotation of the rotor of the joint motor will inevitably increase the probability of actuator failure, which will further affect the manipulation stability and control accuracy of the space manipulator. Therefore, it is of great significance to study the fault-tolerant control of the actuator faults of the space robots. Hu et al [**?**] presents an adaptive robust fault-tolerant controller with finite-time convergence for the redundant spacecraft with momentum flywheel faults. For a class of uncertain time-delay nonlinear systems with actuator faults, Guo and Liang [5] proposed an adaptive decentralized fault-tolerant control algorithm based on time-delay substitution and fuzzy logic systems. For a class of nonlinear systems with random disturbances and Markovian jumping actuator faults, Fan et al [4] designed an adaptive fault-tolerant control scheme. For a class of nonlinear strict-feedback systems with unmeasured states and actuator faults, Tong [21] introduced an observer-based adaptive fuzzy fault-tolerant controller. For a class of stochastic nonstrict-feedback nonlinear systems with input quantization and actuator faults, Ma et al [12] proposes an adaptive fuzzy fault-tolerant controller. For a class of switched networked control systems with external disturbances and actuator/sensor faults, Li and Chen [10] proposed a robust adaptive control method based on fault observer and second-order discrete-time sliding mode function. For a class of surface vessels with actuator saturation and faults, Zheng et al [29] formulated an error-constrained line-of-sight tracking control scheme.

For the space robot with different working conditions, the relevant scholars have developed the corresponding control schemes. Yu [26] proposed a robust controller based on nonlinear state observer for the space robot with unavailable joint angular velocity. For the space robot with dead zone in control input, Huang [9] designed an adaptive anti-dead-zone controller based on dynamic surface technology and fuzzy logic function. For the tethered space robot with saturated control input, Lu et al [11] formulated an adaptive anti-windup controller. It is worth noting that none of these studies have considered the joint actuator gain fault of space robot.

Actuator faults can be divided into gain faults and bias faults. At present, the research on gain fault is very scarce. Since the bias fault can be treated as an external disturbance,

so the research on this kind of fault is very mature. In this paper, the fault-tolerant control of the space robots with joint actuator gain faults is studied. Firstly, the dynamic model of the underactuated space robot is deduced combining conservation law of linear momentum with Lagrange method. Then, the dynamic model of the manipulator joints is obtained by using the mathematical operation of the block matrices. Subsequently, an adaptive sliding mode fault-tolerant control algorithm based on fault observer is proposed for the joint system with gain actuator faults. It is proved that the proposed control algorithm can guarantee the global asymptotic stability of the closed-loop system through Lyapunov theorem. Since the designed fault observer can accurately observe the gain faults, which indicates that the proposed control strategy can provide a theoretical basis for evaluating the on-orbit service life of the space robots.

The main contributions of this work, compared with the current literatures, can be summarized as follows:

(1) Compared with the current neural-network-based fault observer, the adaptive sliding mode fault observer proposed in this paper has the advantages of simple structure and fast calculation speed.

(2) The active fault-tolerant control method based on fault observation formulated in this study has better control effect than the traditional passive control strategies, since it can identify the fault information of the joint actuator, so the operation performance of the space robot can be evaluated conveniently.

2. SYSTEM DESCRIPTION

The structure of the space robot system consist of a free-floating rigid base B_0 and two rigid links B_1 and B_2, as shown in Figure 1. $O - XY$ is the inertial coordinate frame of the system, while $o_i - x_i y_i$ is the local coordinate frame of $B_i (i = 0, 1, 2)$; O_i is the rotation center of $B_i (i = 0, 1, 2)$, while C_i is the mass center of B_i; l_0 is the distance from point O_0 to O_1; $l_i (i = 1, 2)$ is the length of link B_i along the x_i axis; m_i is the mass of $B_i (i = 0, 1, 2)$, and J_i is the inertia moment of B_i with respect to its mass center C_i; θ_0 is attitude angle of the base; $\theta_i (i = 1, 2)$ is the angular displacement of the ith link; The mass of whole system is $M = m_0 + m_1 + m_2$.

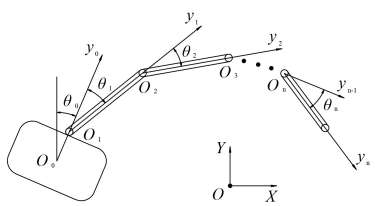

Fig. 1. The structure of free-floating space robot system.

Assumption 1. There is no external force or torque that acts on the system, and thus linear momentum conservation law strictly holds.

The position vector $r_i(i = 0, 1, 2)$ in the local coordinate frame $o_i x_i y_i$ are given by

$$\begin{cases} \boldsymbol{r}_0 = (x_0, y_0)^{\mathrm{T}} \\ \boldsymbol{r}_1 = \boldsymbol{r}_0 + l_0\boldsymbol{e}_0 + a_1\boldsymbol{e}_1 \\ \boldsymbol{r}_2 = \boldsymbol{r}_0 + l_0\boldsymbol{e}_0 + l_1\boldsymbol{e}_1 + a_2\boldsymbol{e}_2 \end{cases} \tag{1}$$

where $\boldsymbol{e}_i$ is the unit vector along the y_i axis, i. e., $\boldsymbol{e}_0 = [\cos(\theta_0), \sin(\theta_0)]^{\mathrm{T}}$, $\boldsymbol{e}_1 = [\cos(\theta_0 + \theta_1), \sin(\theta_0 + \theta_1)]^{\mathrm{T}}$, $\boldsymbol{e}_2 = [\cos(\theta_0 + \theta_1 + \theta_2), \sin(\theta_0 + \theta_1 + \theta_2)]^{\mathrm{T}}$.

It is reasonable to assume that the initial momentum of the system is zero, i. e., $\dot{\boldsymbol{r}}_c = 0$, then according to Assumption 1, we have

$$\sum_{i=0}^{2} m_i \dot{\boldsymbol{r}}_i = M\dot{\boldsymbol{r}}_c = 0 \tag{2}$$

where $\boldsymbol{r}_c$ is the position vector of the mass center of the whole system.

Substituting equation (1) to equation (2), we have

$$\begin{cases} \dot{\boldsymbol{r}}_0 = N_0\dot{\boldsymbol{e}}_0 + N_1\dot{\boldsymbol{e}}_1 + N_2\dot{\boldsymbol{e}}_2 \\ \dot{\boldsymbol{r}}_1 = (N_0 + l_0)\,\dot{\boldsymbol{e}}_0 + (N_1 + a_1)\,\dot{\boldsymbol{e}}_1 + N_2\dot{\boldsymbol{e}}_2 \\ \dot{\boldsymbol{r}}_2 = (N_0 + l_0)\,\dot{\boldsymbol{e}}_0 + (N_1 + l_1)\,\dot{\boldsymbol{e}}_1 + (N_2 + a_2)\,\dot{\boldsymbol{e}}_2 \end{cases} \tag{3}$$

where $N_0 = -(m_1 + m_2)\, l_0/M$, $N_1 = -(m_1 a_1 + m_2 l_1)/M$, $N_2 = -m_2 a_2/M$.

The kinetic energy of $B_i(i = 0, 1, 2)$ is

$$\begin{cases} T_0 = \frac{1}{2} m_0 \dot{\boldsymbol{r}}_0^{\mathrm{T}} \dot{\boldsymbol{r}}_0 + \frac{1}{2} J_0 \dot{\theta}_0^2 \\ T_1 = \frac{1}{2} m_1 \dot{\boldsymbol{r}}_1^{\mathrm{T}} \dot{\boldsymbol{r}}_1 + \frac{1}{2} J_1 \left(\dot{\theta}_0 + \dot{\theta}_1\right)^2 \\ T_2 = \frac{1}{2} m_2 \dot{\boldsymbol{r}}_2^{\mathrm{T}} \dot{\boldsymbol{r}}_2 + \frac{1}{2} J_2 \left(\dot{\theta}_0 + \dot{\theta}_1 + \dot{\theta}_2\right)^2 \end{cases}. \tag{4}$$

Therefore, the kinetic energy of the whole system is

$$T = \sum_{i=0}^{2} T_i. \tag{5}$$

Considering Assumption 1, one can know that the potential energy of the rigid system V is zero. According to Lagrange method, the dynamics equation of the system can be described as

$$\frac{d}{dt}\frac{\partial L}{\partial \dot{\theta}_i} - \frac{\partial L}{\partial \theta_i} = Q_i \tag{6}$$

where $L = T - V = T$ denotes the Langrange function, and Q_i represents the generalized force or torques delivered by joint actuators. Equation (6) can be rewritten in the form of differential equation as

$$\boldsymbol{D}(\boldsymbol{q})\ddot{\boldsymbol{q}} + \boldsymbol{H}(\boldsymbol{q}, \dot{\boldsymbol{q}})\dot{\boldsymbol{q}} = \begin{bmatrix} 0 \\ \boldsymbol{\tau} \end{bmatrix} \tag{7}$$

where $\boldsymbol{q} = [\theta_0\ \theta_1\ \theta_2\ ]^T$ is the state variables; $\boldsymbol{D}(\boldsymbol{q}) \in \boldsymbol{R}^{3\times 3}$ is the symmetric and positive-definite inertial matrix, and $\boldsymbol{H}(\boldsymbol{q}, \dot{\boldsymbol{q}})\dot{\boldsymbol{q}} \in \boldsymbol{R}^3$ is the Coriolis/centrifugal force vector (see Appendix for detailed dynamics parameters); $\boldsymbol{\tau} = [u_1\ u_2]^T$ is the control inputs.

Property 1. $\dot{\boldsymbol{D}}(\boldsymbol{q}) - 2\boldsymbol{H}(\boldsymbol{q}, \dot{\boldsymbol{q}})$ is a skew symmetric matrix, i. e.,

$$\boldsymbol{\psi}^T[\dot{\boldsymbol{D}}(\boldsymbol{q}) - 2\boldsymbol{H}(\boldsymbol{q}, \dot{\boldsymbol{q}})]\boldsymbol{\psi} = 0, \quad \forall \boldsymbol{\psi} \in R^3.$$

In order to obtain the dynamic model of joints, the dynamic model (7) can be expressed as

$$\begin{bmatrix} D_{11} & \boldsymbol{D}_{12} \\ \boldsymbol{D}_{21} & \boldsymbol{D}_{22} \end{bmatrix} \begin{bmatrix} \ddot{q}_b \\ \ddot{\boldsymbol{q}}_r \end{bmatrix} + \begin{bmatrix} H_{11} & \boldsymbol{H}_{12} \\ \boldsymbol{H}_{21} & \boldsymbol{H}_{22} \end{bmatrix} \begin{bmatrix} \dot{q}_b \\ \dot{\boldsymbol{q}}_r \end{bmatrix} = \begin{bmatrix} 0 \\ \boldsymbol{\tau} \end{bmatrix} \tag{8}$$

where D_{11}, $\boldsymbol{D}_{12} = \boldsymbol{D}_{21} \in \boldsymbol{R}^{1\times 2}$ and $\boldsymbol{D}_{22} \in \boldsymbol{R}^{2\times 2}$ are the sub-matrices of $\boldsymbol{D}$; H_{11}, $\boldsymbol{H}_{12} \in \boldsymbol{R}^{1\times 2}$, $\boldsymbol{H}_{21} \in \boldsymbol{R}^{2\times 1}$ and $\boldsymbol{H}_{22} \in \boldsymbol{R}^{2\times 2}$ are the sub-matrices of $\boldsymbol{H}$; $q_b = \theta_0$, $\boldsymbol{q}_r = [\theta_1\ \theta_2]^T$. Further, from equation (8), we have

$$D_{11}\ddot{q}_b + \boldsymbol{D}_{12}\ddot{\boldsymbol{q}}_r + H_{11}\dot{q}_b + \boldsymbol{H}_{12}\dot{\boldsymbol{q}}_r = 0 \tag{9}$$

$$\boldsymbol{D}_{21}\ddot{q}_b + \boldsymbol{D}_{22}\ddot{\boldsymbol{q}}_r + \boldsymbol{H}_{21}\dot{q}_b + \boldsymbol{H}_{22}\dot{\boldsymbol{q}}_r = \boldsymbol{\tau}. \tag{10}$$

Solving equation (9) for $\ddot{q}_b$

$$\ddot{q}_b = -D_{11}^{-1}\left(\boldsymbol{D}_{12}\ddot{\boldsymbol{q}}_r + H_{11}\dot{q}_b + \boldsymbol{H}_{12}\dot{\boldsymbol{q}}_r\right). \tag{11}$$

Combining equations (10) with (11), one can obtain the so-called dynamic equation of the joints as follows

$$\overline{\boldsymbol{D}}(q)\ddot{\boldsymbol{q}}_r + \overline{\boldsymbol{C}}(\boldsymbol{q}, \boldsymbol{q}) = \boldsymbol{\tau}. \tag{12}$$

where $\overline{\boldsymbol{D}} = \boldsymbol{D}_{22} - \boldsymbol{D}_{21}D_{11}^{-1}\boldsymbol{D}_{12}$, $\overline{\boldsymbol{C}} = \left(\boldsymbol{H}_{21} - \boldsymbol{D}_{21}D_{11}^{-1}H_{11}\right)\dot{q}_b + \left(\boldsymbol{H}_{22} - \boldsymbol{D}_{21}D_{11}^{-1}\boldsymbol{H}_{12}\right)\dot{\boldsymbol{q}}_r$. For the convenience of the design of the subsequent controller, according to the Quasi-linearization theory [26], equation (12) can be rewritten as

$$\overline{\boldsymbol{D}}(q)\ddot{\boldsymbol{q}}_r + \overline{\boldsymbol{H}}(\boldsymbol{q})\dot{\boldsymbol{q}}_r + \left(\overline{\boldsymbol{C}}(\boldsymbol{q}, \boldsymbol{q}) - \overline{\boldsymbol{H}}(\boldsymbol{q})\dot{\boldsymbol{q}}_r\right) = \boldsymbol{\tau} \tag{13}$$

where $\overline{H}_{ij} = \sum_{k=1}^{2} \frac{1}{2}\left(\frac{\partial \overline{D}_{ij}}{\partial q_{r(k-1)}} + \frac{\partial \overline{D}_{ik}}{\partial q_{r(j-1)}} - \frac{\partial \overline{D}_{jk}}{\partial q_{r(i-1)}}\right)\dot{q}_{r(k-1)}$ When the joint actuator gain fault occurs [27], the joint dynamics model (13) can be described by

$$\overline{\boldsymbol{D}}(q)\ddot{\boldsymbol{q}}_r + \overline{\boldsymbol{H}}(\boldsymbol{q}, \dot{\boldsymbol{q}})\dot{\boldsymbol{q}}_r + \left(\overline{\boldsymbol{C}}(\boldsymbol{q}, \dot{\boldsymbol{q}}) - \overline{\boldsymbol{H}}(\boldsymbol{q}, \dot{\boldsymbol{q}})\dot{\boldsymbol{q}}_r\right) = \boldsymbol{\Lambda}\boldsymbol{\tau} \tag{14}$$

where $\boldsymbol{\Lambda} = diag\{\lambda_1, \lambda_2\}$ denotes the actuator gain fault matrix which is supposed to be unknown with $0 < \lambda_i \leq 1$, indicates the remaining control rate of the ith actuator. The case $\lambda_i = 1$ stands for that the ith actuator is fault-free, while $0 < \lambda_i < 1$ means that the ith actuator loses its effectiveness partially. The main contribution of this research is to formulate a observer-based fault-tolerant control algorithm for the joint dynamics model (14) under the actuator gain fault, so as to realize trajectory tracking control and actuator gain fault observation.

3. FAULT-TOLERANT CONTROLLER DESIGN

Since the dynamic model (14) represents the actual physical system, then $\overline{\boldsymbol{D}}$ is a positive-definite matrix.

In order to facilitate the design of the subsequent control algorithm, equation (14) can be rewritten as

$$\ddot{\boldsymbol{q}}_r = \overline{\boldsymbol{D}}^{-1}\boldsymbol{\Lambda}\boldsymbol{\tau} - \overline{\boldsymbol{D}}^{-1}\boldsymbol{\varphi}(\boldsymbol{q},\dot{\boldsymbol{q}}) - \overline{\boldsymbol{D}}^{-1}\overline{\boldsymbol{H}}(\boldsymbol{q},\dot{\boldsymbol{q}})\dot{\boldsymbol{q}}_r \tag{15}$$

where $\varphi(\boldsymbol{q},\dot{\boldsymbol{q}}) = \overline{\boldsymbol{C}}(\boldsymbol{q},\dot{\boldsymbol{q}}) - \overline{\boldsymbol{H}}(\boldsymbol{q},\dot{\boldsymbol{q}})\dot{\boldsymbol{q}}_r$

Assumption 2. Desired trajectories $\boldsymbol{q}_{rd}$, $\dot{\boldsymbol{q}}_{rd}$ and $\ddot{\boldsymbol{q}}_{rd}$ are norm-bounded.

Define the trajectory tracking error as $\boldsymbol{e} = \boldsymbol{q}_r - \boldsymbol{q}_{rd}$. Then, the extended error is selected

$$\boldsymbol{S} = \dot{\boldsymbol{e}} + \varepsilon\boldsymbol{e} \tag{16}$$

where ε is a positive constant. Differentiating (16) with respect to time t, and utilizing equation (15) yields

$$\dot{\boldsymbol{S}} = \overline{\boldsymbol{D}}^{-1}\boldsymbol{P}\boldsymbol{\tau} - \overline{\boldsymbol{D}}^{-1}\boldsymbol{\varphi} - \left(\overline{\boldsymbol{D}}^{-1}\overline{\boldsymbol{H}}\dot{\boldsymbol{q}}_r + \ddot{\boldsymbol{q}}_{rd} - \varepsilon\dot{\boldsymbol{e}}\right). \tag{17}$$

The sliding mode fault-tolerant controller (SMFTC) is designed as

$$\boldsymbol{\tau} = \hat{\boldsymbol{\Lambda}}^{-1}\overline{\boldsymbol{D}}\left(\left[-k_{11}\sqrt{|S_1|}\,\mathrm{sgn}\,S_1, -k_{12}\sqrt{|S_2|}\,\mathrm{sgn}\,S_2\right]^{\mathrm{T}} + \boldsymbol{v} + \left(\overline{\boldsymbol{D}}^{-1}\overline{\boldsymbol{H}}\dot{\boldsymbol{q}}_{\boldsymbol{r}} + \ddot{\boldsymbol{q}}_{rd} - \varepsilon\dot{\boldsymbol{e}}\right)\right) \tag{18}$$

where variables $\boldsymbol{v}$ and $\boldsymbol{\Lambda}$ are adjusted adaptively by

$$\dot{\boldsymbol{v}} = -\frac{1}{2}\left[k_{21}\,\mathrm{sgn}\,S_1, k_{22}\,\mathrm{sgn}\,S_2\right]^{\mathrm{T}} \tag{19}$$

$$\dot{\hat{\boldsymbol{\Lambda}}} = \alpha\Gamma\left(\overline{\boldsymbol{D}}^{-1}\right)^{\mathrm{T}}\left[\mathrm{sgn}\,S_1, \mathrm{sgn}\,S_2\right]^{\mathrm{T}}\boldsymbol{\tau}^{\mathrm{T}} \tag{20}$$

where k_{11}, k_{12}, k_{21}, k_{11}, α and Γ are positive constants; $\hat{\boldsymbol{\Lambda}} = diag\{\hat{\lambda}_1, \hat{\lambda}_2\}$ is the estimation of $\boldsymbol{\Lambda}$. Substituting equation (18) into equation (17), one obtains

$$\dot{\boldsymbol{S}} = \overline{\boldsymbol{D}}^{-1}\tilde{\boldsymbol{\Lambda}}\boldsymbol{\tau} - \left[k_{11}\sqrt{S_1}\,\mathrm{sgn}\,S_1, k_{12}\sqrt{|S_2|}\,\mathrm{sgn}\,S_2\right]^{\mathrm{T}} + \boldsymbol{\sigma} \tag{21}$$

where $\tilde{\boldsymbol{\Lambda}} = \boldsymbol{\Lambda} - \hat{\boldsymbol{\Lambda}}$, $\quad \boldsymbol{\sigma} = \boldsymbol{v} - \overline{\boldsymbol{D}}^{-1}\boldsymbol{\varphi} = [\sigma_1, \sigma_2]^{\mathrm{T}}$. Defining $\overline{\boldsymbol{D}}^{-1}\tilde{\boldsymbol{\Lambda}}\boldsymbol{\tau} = [\mu_1, \mu_2]^{\mathrm{T}}$, and differentiating $\boldsymbol{\sigma}$ with respect to time t, we have

$$\dot{\boldsymbol{\sigma}} = -\frac{1}{2}\left[k_{21}\,\mathrm{sgn}\,S_1, k_{22}\,\mathrm{sgn}\,S_2\right]^{\mathrm{T}} + \boldsymbol{\xi} \tag{22}$$

where $\boldsymbol{\xi} = -\dot{\overline{\boldsymbol{D}}}^{-1}\boldsymbol{\varphi} - \overline{\boldsymbol{D}}^{-1}\dot{\boldsymbol{\varphi}} = [\xi_1, \xi_2]^{\mathrm{T}}$.

4. STABILITY ANALYSIS

Theorem 4.1. Consider the joint dynamics system (12) with Assumptions 1 and 2. If the fault-tolerant control law is designed as equation (18), with the adaptive laws (19) and (20), then the closed-loop system (21) is globally asymptotically stable, i. e.,

$$\lim_{t\to\infty} \boldsymbol{e} = 0 \tag{23}$$

P r o o f . In order to obtain the subsequent Lyapunov function, define

$$\boldsymbol{z} = \left[\boldsymbol{z}_1^{\mathrm{T}}\ , \boldsymbol{z}_2^{\mathrm{T}}\right]^{\mathrm{T}} = [z_{11}, z_{12}, z_{21}, z_{22}]^{\mathrm{T}} = \left[\sqrt{|S_1|}\,\mathrm{sgn}\,S_1, \sqrt{|S_2|}\,\mathrm{sgn}\,S_2, \sigma_1, \sigma_2\right]^{\mathrm{T}}. \tag{24}$$

Differentiating equation (24) with respect to time t leads to [28]

$$\begin{cases} \dot{z}_{1i} = -\frac{1}{2|z_{1i}|}\left(k_{1i}z_{1i} - z_{2i} - \mu_i\right) \\ \dot{z}_{2i} = -\frac{1}{2|z_{1i}|}k_{2i}z_{1i} + \xi_i \end{cases} \tag{25}$$

where ξ_i(i=1,2) can be expressed as

$$\xi_i = \frac{\rho_i}{2}\,\mathrm{sgn}\,S_i = \frac{\rho_i}{2}\,\frac{z_{1i}}{|z_{1i}|}, \quad 0 < \rho_i \le 2\delta_i \tag{26}$$

where ρ_i and δ_i are positive constants. Substituting equation (26) into equation (25) yields

$$\dot{\boldsymbol{z}} = \boldsymbol{A}\boldsymbol{z} + \boldsymbol{B} \tag{27}$$

where $\boldsymbol{A} = \begin{bmatrix} -\frac{k_{11}}{2|z_{11}|} & 0 & \frac{1}{2|z_{11}|} & 0 \\ 0 & -\frac{k_{12}}{2|z_{12}|} & 0 & \frac{1}{2|z_{12}|} \\ -\frac{k_{21}-\rho_1}{2|z_{11}|} & 0 & 0 & 0 \\ 0 & -\frac{k_{22}-\rho_2}{2|z_{12}|} & 0 & 0 \end{bmatrix}$, $\boldsymbol{B} = \frac{1}{2}\begin{bmatrix} \boldsymbol{R} & \boldsymbol{0} \\ \boldsymbol{0} & \boldsymbol{0} \end{bmatrix}\begin{bmatrix} \overline{\boldsymbol{D}}^{-1}\tilde{\boldsymbol{\Lambda}}\boldsymbol{\tau} \\ \boldsymbol{0} \end{bmatrix}$,
$\boldsymbol{R} = \mathrm{diag}\left\{\frac{1}{|z_{11}|}, \frac{1}{|z_{12}|}\right\}$ Choosing the Lyapunov candidate as

$$\boldsymbol{V} = \boldsymbol{z}^{\mathrm{T}}\boldsymbol{P}\boldsymbol{z} + \frac{1}{2}\,\mathrm{tr}\left(\tilde{\boldsymbol{\Lambda}}^{\mathrm{T}}\Gamma^{-1}\tilde{\boldsymbol{\Lambda}}\right) \tag{28}$$

where tr$(\cdot)$ denotes the trace of matrix $(\cdot)$; $\boldsymbol{P} = \begin{bmatrix} \alpha\boldsymbol{I}_{2\times2} & \boldsymbol{0} \\ \boldsymbol{0} & \beta\boldsymbol{I}_{2\times2} \end{bmatrix} = \begin{bmatrix} \boldsymbol{P}_{11} & \boldsymbol{0} \\ \boldsymbol{0} & \boldsymbol{P}_{22} \end{bmatrix}$,
$\boldsymbol{I}$ denotes the identity matrix, and β is a positive constant.

Differentiating equation (28) with respect to time t, and considering equation (27), we have

$$\dot{V} = -\boldsymbol{z}^{\mathrm{T}}\boldsymbol{Q}\boldsymbol{z} + 2\boldsymbol{B}^{\mathrm{T}}\boldsymbol{P}\boldsymbol{z} - \mathrm{tr}\left(\tilde{\boldsymbol{\Lambda}}^{\mathrm{T}}\Gamma^{-1}\dot{\tilde{\boldsymbol{\Lambda}}}\right) \tag{29}$$

where $\boldsymbol{Q} = -\left(\boldsymbol{A}^{\mathrm{T}}\boldsymbol{P} + \boldsymbol{P}\boldsymbol{A}\right) = \begin{bmatrix} \boldsymbol{Q}_{11} & \boldsymbol{Q}_{12} \\ \boldsymbol{Q}_{12} & \boldsymbol{Q}_{22} \end{bmatrix}$, $\boldsymbol{Q}_{11} = \begin{bmatrix} \frac{k_{11}\alpha}{|z_{11}|} & 0 \\ 0 & \frac{k_{12}\alpha}{|z_{12}|} \end{bmatrix}$, $\boldsymbol{Q}_{22} = \begin{bmatrix} 0 & 0 \\ 0 & 0 \end{bmatrix}$,
$\boldsymbol{Q}_{12} = \begin{bmatrix} \frac{(k_{21}-\rho_1)\beta-\alpha}{2|z_{11}|} & 0 \\ 0 & \frac{(k_{22}-\rho_2)\beta-\alpha}{2|z_{12}|} \end{bmatrix}$.

Since

$$\boldsymbol{z}^{\mathrm{T}}\boldsymbol{Q}\boldsymbol{z} = \boldsymbol{z}_1^{\mathrm{T}}\boldsymbol{Q}_{11}\boldsymbol{z}_1 + \boldsymbol{z}_2^{\mathrm{T}}\boldsymbol{Q}_{12}\boldsymbol{z}_1 + \boldsymbol{z}_1^{\mathrm{T}}\boldsymbol{Q}_{12}\boldsymbol{z}_2. \tag{30}$$

If $\boldsymbol{Q}$ is a positive semi-definite matrix, then

$$\begin{cases} k_{1i}\alpha > 0 \\ (k_{2i} - \rho_i)\,\beta - \alpha = 0 \end{cases}. \tag{31}$$

From equation (31),we have

$$\begin{cases} k_{1i} > 0 \\ k_{2i} = \frac{\alpha}{\beta} + \rho_i \end{cases}. \tag{32}$$

Substituting equation (32) into equation (30) yields

$$\boldsymbol{z}^{\mathrm{T}}\boldsymbol{Q}\boldsymbol{z} = \boldsymbol{z}_1^{\mathrm{T}}\boldsymbol{Q}_{11}\boldsymbol{z}_1. \tag{33}$$

Combining equation (33) and adaptive law (20), equation (29) can be rewritten as

$$\dot{V} = -\boldsymbol{z}_1^{\mathrm{T}}\boldsymbol{Q}_{11}\boldsymbol{z}_1 \leq -\lambda_{\min}\left\{\boldsymbol{Q}_{11}\right\}\left|\boldsymbol{z}_1\right|^2 \tag{34}$$

where $\lambda_{\min}\left\{\boldsymbol{Q}_{11}\right\}$ represents the minimum eigenvalue of matrix $\boldsymbol{Q}_{11}$.

From equation (34), one has $V \in L_\infty$; hence utilizing equation (28), we can know that $\boldsymbol{z}_1 \in L_\infty$, $\boldsymbol{z}_2 \in L_\infty$ and $\tilde{\boldsymbol{\Lambda}} \in L_\infty$; further, from equation (25), we get $\dot{\boldsymbol{z}}_1 \in L_\infty$ and $\dot{\boldsymbol{z}}_2 \in L_\infty$. According to Barbalat lemma, one obtains

$$\lim_{t\to\infty} \boldsymbol{z}_1 = 0. \tag{35}$$

Therefore, combining equations (16) and (24), we have

$$\lim_{t\to\infty} \boldsymbol{e} = 0 \tag{36}$$

which implies the closed-loop system (21) satisfies global asymptotic stability and this completes the proof of Theorem 4.1.

□

5. SIMULATION EXAMPLES

In order to illustrate the fault-tolerant performance of the proposed SMFTC algorithm (18), numerical simulations are conducted. The simulation results in different working condition of controller (18) are compared with those of the computed torque controller (CTC) proposed by [29], which can not address the actuator gain fault. The CTC algorithm is described by

$$\boldsymbol{\tau}_{CTC} = \overline{\boldsymbol{D}}\left(\ddot{\boldsymbol{q}}_d - k_v\dot{\boldsymbol{e}} - k_p\boldsymbol{e}\right) + \overline{\boldsymbol{C}} \tag{37}$$

where k_v and k_p are positive constant.

The physical parameters assigned on the space robot system are $l_0 = 1\mathrm{m}$, $l_1 = l_2 = 3\mathrm{m}$, $m_0 = 40\mathrm{kg}$, $m_1 = m_2 = 3\mathrm{kg}$, $J_0 = 40\mathrm{kg}\cdot\mathrm{m}^2$,$J_1 = J_2 = 1\mathrm{kg}\cdot\mathrm{m}^2$.

The controller parameters of SMFTC algorithm are set as $k_{11} = 0.15$, $k_{12} = 0.8$, $k_{21} = 0.1$, $k_{22} = 0.2$, $\alpha = 4.5$, $\Gamma = 0.1$, $\varepsilon = 3$; and CTC algorithm are $k_v = 6$, $k_p = 10$.

The desired trajectories of the link joints are $\theta_{1\mathrm{d}} = \sin(0.2\pi t), \theta_{2\mathrm{d}} = \cos(0.2\pi t)$.

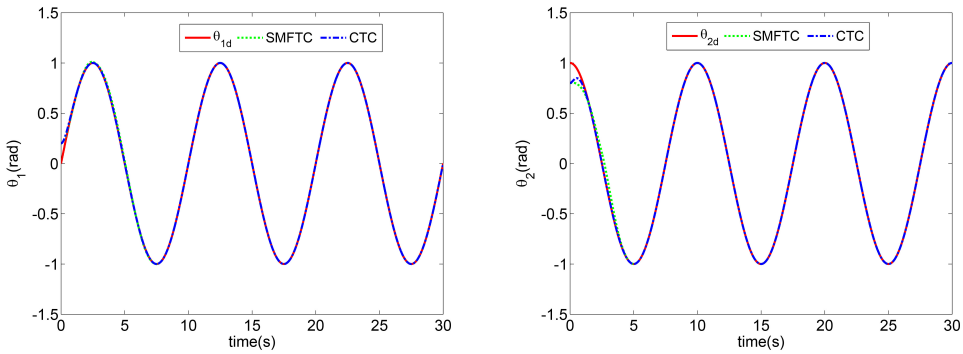

(a) link 1 (b) link 2

Fig. 2. Time response of the joint tracking trajectory.

5.1. Time response in actuator fault-free case

In this case, no joint actuators fault occurs, i. e., $\mathbf{\Lambda} = \text{diag}\{1, 1\}$. The initial values of the observer are $\boldsymbol{v}(0) = [0.1, 0.1]^{\mathrm{T}}$, $\widehat{\mathbf{\Lambda}}(0) = [1.5, 1.5]^{\mathrm{T}}$. The simulation results are shown in Figures 2 to 4. Time response of the joint tracking trajectory of the SMFTC algorithm and the CTC algorithm is show in Figure 2, while Figure 3 is the time response of the sliding manifold S. The joint actuator gain fault and its estimation is presented in Figure 4.

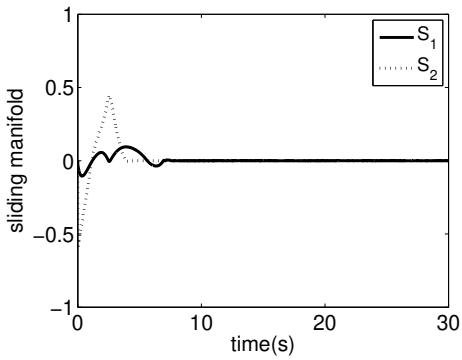

Fig. 3. Time response of the sliding manifold S.

It can be seen that both the SMFTC algorithm and CTC algorithm can stabilize the tracking error system, as shown in Figure 2; From Figure 4, one can observe that the joint actuator gain fault can be observed accurately and promptly.

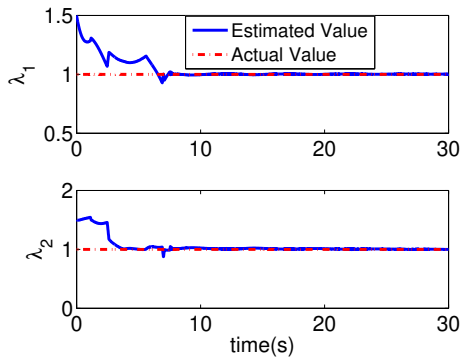

Fig. 4. Gain fault and its estimation.

5.2. Time response in the case of actuator faults

In this case, the actuator gain fault scenarios are taken into account. The actuator joint 1 loses 70% of its normal control power at 10s, while the joint 2 actuator loses 40% normal power at 15s; i. e.

$$\lambda_1 = \begin{cases} 1, & 0\text{s} \le t < 10\text{s} \\ 0.3, & 10\text{s} < t \le 30\text{s} \end{cases}, \quad \lambda_2 = \begin{cases} 1, & 0\text{s} \le t < 15\text{s} \\ 0.6, & 15\text{s} \le t < 30\text{s} \end{cases}. \tag{38}$$

The initial values of the observer are $\boldsymbol{v}(0) = [0.1, 0.1]^{\mathrm{T}}$, $\widehat{\boldsymbol{\Lambda}}(0) = [0.5, 0.8]^{\mathrm{T}}$. The simulation results are shown in Figures 5 to 7. Time response of the joint tracking trajectory of the two algorithms is shown in Figure 5, while Figure 6 is the time response of the sliding manifold S. The joint actuator gain fault and its estimation is presented in Figure 7.

One can observe that once all the joint actuators are subjected to the gain faults, significant trajectory tracking errors can be seen when CTC algorithm is utilized to the system as shown in Figure 5, since the CTC algorithm do not has the mechanism to resist the actuator gain fault. While the proposed SMFTC algorithm can still ensures that the states of the tracking error system reach the sliding manifold as depicted in Figure 6. From Figure 7, one can observe that the the joint actuator gain fault can still be estimated accurately under the fault mode.

6. CONCLUSION

The fault-tolerant control of the underactuated space robots with joint actuator gain faults is studied. The dynamic model of the space robot is deduced combining conservation law of linear momentum with Lagrange method. Based on the system dynamic model, the joint dynamic model is obtained by using the mathematical operation of the block matrices. An adaptive sliding mode fault-tolerant control algorithm based on the fault observer is proposed for the joint system with gain actuator faults. The simulation results show that the proposed fault-tolerant algorithm is robust to actuator gain faults.

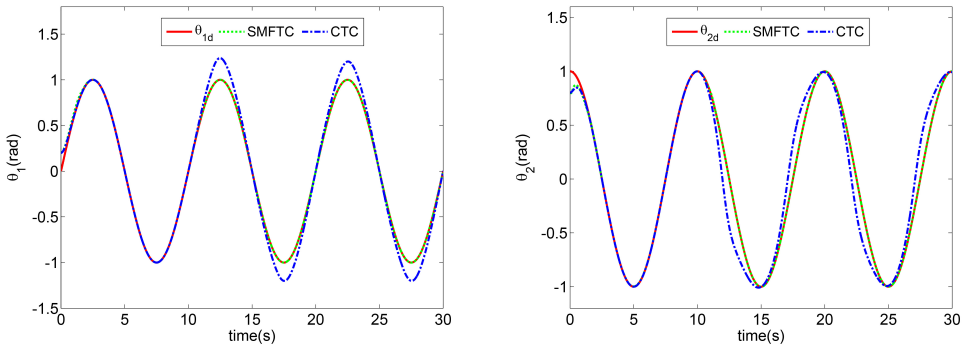

(a) link 1 (b) link 2

Fig. 5. Time response of the joint tracking trajectory.

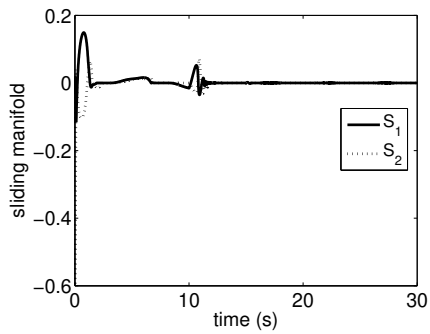

Fig. 6. Time response of the sliding manifold S.

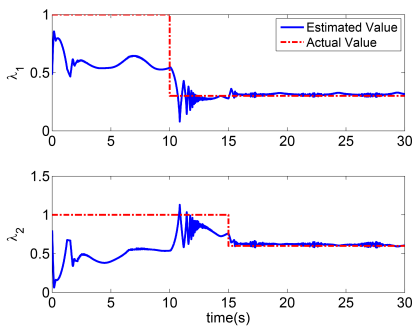

Fig. 7. Gain fault and its estimation.

Since the designed fault observer can accurately observe the gain faults, which indicates that the proposed control strategy can provide a theoretical basis for evaluating the on-orbit service life of the space robots. The control algorithm does not need to measure and feedback the angular acceleration of the base attitude and has few adaptive variables, hence it has great value in engineering application. In the future, the author will extend the fault-tolerant algorithm to the motion control of the space robots with flexible manipulators and flexible joints simultaneously.

ACKNOWLEDGEMENT

This work was partially supported supported by National Natural Science Fundation of China (11372073, 11072061).

APPENDIX

The dynamics parameters of floating-based space robot system

$D(1,1) = 2\left[E_1 + E_2 + E_3 + E_4\cos(\theta_1) + E_5\cos(\theta_1+\theta_2) + E_6\cos(\theta_2)\right]$,
$D(1,2) = 2E_2 + 2E_3 + E_4\cos(\theta_1) + E_5\cos(\theta_1+\theta_2) + 2E_6\cos(\theta_2)$,
$D(1,3) = 2E_3 + E_5\cos(\theta_1+\theta_2) + E_6\cos(\theta_2)$, $D(2,1) = D(1,2)$,
$D(2,2) = 2E_2 + 2E_3 + 2E_6\cos(\theta_2)$, $D(2,3) = 2E_3 + E_6\cos(\theta_2)$,
$D(3,1) = D(1,3)$, $D(3,2) = D(2,3)$, $D(3,3) = 2E_3$;
$H(1,1) = -E_4\dot{\theta}_1\sin(\theta_1) - E_5\left(\dot{\theta}_1+\dot{\theta}_2\right)\sin(\theta_1+\theta_2) - E_6\dot{\theta}_2\sin(\theta_2)$,
$H(1,2) = -2E_4\left(\dot{\theta}_0+\dot{\theta}_1\right)\sin(\theta_1) - E_5\left(\dot{\theta}_1+\dot{\theta}_2\right)\sin(\theta_1+\theta_2) - E_6\dot{\theta}_2\sin(\theta_2)$,
$H(1,3) = -E_5\left(\dot{\theta}_0+\dot{\theta}_1+\dot{\theta}_2\right)\sin(\theta_1+\theta_2) - E_6\left(\dot{\theta}_0+\dot{\theta}_1+\dot{\theta}_2\right)\sin(\theta_2)$,
$H(2,1) = E_5\dot{\theta}_0\sin(\theta_1+\theta_2) - E_6\dot{\theta}_2\sin(\theta_2)$, $H(2,2) = E_4\dot{\theta}_0\sin(\theta_1) - E_6\dot{\theta}_2\sin(\theta_2)$,
$H(2,3) = -E_6\left(\dot{\theta}_0+\dot{\theta}_1+\dot{\theta}_2\right)\sin(\theta_2)$, $H(3,1) = E_5\dot{\theta}_0\sin(\theta_1+\theta_2) + E_6\left(\dot{\theta}_0+\dot{\theta}_1\right)\sin(\theta_2)$,
$H(3,2) = E_6\left(\dot{\theta}_0+\dot{\theta}_1\right)\sin(\theta_2)$, $H(3,3) = 0$

where,
$E_1 = \frac{1}{2}\left[m_0N_0^2 + m_1(N_0+l_0)^2 + m_2(N_0+l_0)^2 + J_0\right]$,
$E_2 = \frac{1}{2}\left[m_0N_1^2 + m_1(N_1+d_1)^2 + m_2(N_1+l_1)^2 + J_1\right]$,
$E_3 = \frac{1}{2}\left[m_0N_2^2 + m_1(N_1+l_1)^2 + m_2(N_2+d_2)^2 + J_2\right]$,
$E_4 = m_0N_0N_1 + m_1(N_0+l_0)(N_1+d_1) + m_2(N_0+l_0)(N_1+l_1)$,
$E_5 = m_0N_0N_2 + m_1(N_0+l_0)N_2 + m_2(N_0+l_0)(N_2+d_2)$,
$E_6 = m_0N_1N_2 + m_1(N_1+d_1)N_2 + m_2(N_1+l_1)(N_2+d_2)$.

(Received October 19, 2019)

REFERENCES

[1] L. Angel and J. Viala : Tracking control for robotic manipulators using fractional order controllers with computed torque control. IEEE Latin America Trans. *16* (2018), 1884–1891. DOI:10.1109/TLA.2018.8447353

[2] P. Chutiphon: Robust optimal PID controller design for attitude stabilization of flexible spacecraft. Kybernetika *54* (2018), 1049–1070. DOI:10.14736/kyb-2018-5-1049

[3] P. Chutiphon and J. Anuchit: Disturbance observer-based second order sliding mode attitude tracking control for flexible spacecraft. Kybernetika *53* (2017), 653–678. DOI:10.14736/kyb-2017-4-0653

[4] H. J. Fan, B. Liu, W. Wang, and C. Y. Wen: Adaptive fault-tolerant stabilization for nonlinear systems with Markovian jumping actuator failures and stochastic noises. Automatica *51* (2015), 200–209. DOI:10.1016/j.automatica.2014.10.084

[5] T. Guo and W. S. Chen: Adaptive fuzzy decentralised fault-tolerant control for uncertain non-linear large-scale systems with unknown time-delay. IET Control Theory Appl. *10* (2016), 3427–3446.DOI:10.1049/iet-cta.2016.0471

[6] W. He and Y. T. Dong: Adaptive fuzzy neural network control for a constrained robot using impedance learning. IEEE Trans. Neural Networks Learning Systems *29* (2018), 1174–1186. DOI:10.1109/TNNLS.2017.2665581

[7] W. He, X. He, M. Zou, and H. Li: PDE model-based boundary control design for a flexible robotic manipulator with input backlash. IEEE Trans. Control Systems Technol. *27* (2019), 790–797.DOI:10.1109/TCST.2017.2780055

[8] Q. L. Hu, X. Huo, and B. Xiao: Reaction wheel fault tolerant control for spacecraft attitude stabilization with finite-time convergence. Int. J. Robust Nonlinear Control *23* (2013), 1737–1752. DOI:10.1002/rnc.2924

[9] X. Q., Huang and L. Chen: Anti-dead-zone control based on dynamic surface for space robot with flexible links and elastic base. J. Harbin Engineering University *40* (2019), 2063-2069.

[10] M. Li and Y. Chen: Robust adaptive sliding mode control for switched networked control systems with disturbance and faults. IEEE Trans. Industrial Inform. *15* (2019), 193–204. DOI:10.1109/TII.2018.2808921

[11] Y. B. Lu, P. F. Huang, and Z. J. Meng: Adaptive anti-windup control of post-capture combination via tethered space robot. Advances Space Res. *64* (2019), 847–860. DOI:10.1016/j.asr.2019.05.029

[12] H. Ma, Q. Zhou, L. Bai, and H. J. liang: Observer-based adaptive fuzzy fault-tolerant control for stochastic nonstrict-feedback nonlinear systems with input quantization. IEEE Trans. Systems Man Cybernet.: Systems *49* (2019), 287–298. DOI:10.1109/TSMC.2018.2833872

[13] D. S. Meng, Y. She, W. F Xu, W. N Lu, and B. Liang: Dynamic modeling and vibration characteristics analysis of flexible-link and flexible-joint space manipulator. Multibody System Dynamics *43* (2018), 321–347. DOI:10.1007/s11044-017-9611-6

[14] S. A. A. Moosavian and E. Papadopoulos: Explicit dynamics of space free-flyers with multiple manipulators via spacemaple. Advanced Robotics *18* (2004), 223–244.DOI:10.1163/156855304322758033

[15] Z. Y. Ni, J. G. Liu, Z. G. Wu, and X. H. Shen: Identification of the state-space model and payload mass parameter of a flexible space manipulator using a recursive subspace tracking method. Chinese J. Aeronautics *32* (2019), 513–530. DOI:10.1016/j.cja.2018.05.005

[16] E. Papadopoulos and S. Dubowsky: On the nature of control algorithms for free-floating space manipulators. IEEE Trans. Robotics Automation *7* (1991), 750–758. DOI:10.1109/70.105384

[17] A. Pisculli, L. Felicetti , P. Gasbarri, G. B. Palmerini, and M. Sabatini: A reaction-null/Jacobian transpose control strategy with gravity gradient compensation for on-orbit space manipulators. Aerospace Science Technol. *38* (2014), 30–40. DOI:10.1016/j.ast.2014.07.012

[18] Q. K. Shen, B. Jiang, and C. Vincent: Fault-tolerant control for T-S fuzzy systems with application to near-space hypersonic vehicle with actuator faults. IEEE Trans. Fuzzy Systems *20* (2012), 652–665. DOI:10.1109/TFUZZ.2011.2181181

[19] Y. Shtessel, M. Taleb, and F. Plestan: A novel adaptive-gain supertwisting sliding mode controller: methodology and application. Automatica *48* (2012), 759–769. DOI:10.1016/j.automatica.2012.02.024

[20] J. Slotine and W. Li: On the adaptive control of robot manipulators. Int. J. Robotics Research *6* (1987), 49–59. DOI:10.1177/027836498700600303

[21] S. C. Tong, B. Y. Huo, and Y. M. Li: Observer-based adaptive decentralized fuzzy fault-tolerant control of nonlinear large-scale systems with actuator failures. IEEE Trans. Fuzzy System *22* (2014), 1–15. DOI:10.1109/TFUZZ.2013.2241770

[22] Y. Umetani and K. Yoshida: Continuous path control of space manipulators mounted on OMV. Acta Astronautica *15* (1987), 981–986. DOI:10.1016/0094-5765(87)90022-1

[23] Y. Umetani and K. Yoshida: Resolved motion rate control of space manipulators with generalized Jacobian matrix. IEEE Trans. Robotics Automat. *5* (1989), 303–314.

[24] Z. Vafa and S. Dubowsky: On the Dynamics of Space Manipulators Using the Virtual Manipulator, with Applications to Path Planning. J. Astronautical Sci. *38* (1990), 441–472.

[25] Z. Vafa and S. Dubowsky: The Kinematics and Dynamics of Space Manipulators: The Virtual Manipulator Approach. Int. J. Robotics Res. *9* (1990), 3–21.DOI:10.1177/027836499000900401

[26] X. Y. Yu and L. Chen: Observer Based Robust Control and Vibration Control for a Free-floating flexible Space Manipulator. J. Mechanical Engrg. *52* (2016), 28–35.DOI:10.3901/JME.2016.15.028

[27] Q. Zhang, L. Ji, D. S. Zhou, and X. P. Wei: Nonholonomic motion planning for minimizing base disturbances of space manipulators based on multi-swarm PSO. Robotica *35* (2017), 861–875. DOI:10.1017/S0263574715000855

[28] J. L. Zhao, S. Z. Yan, and J. N. Wu: Analysis of parameter sensitivity of space manipulator with harmonic drive based on the revised response surface method. Acta Astronautica *98* (2014), 86–96.

[29] Z. W. Zheng, L. Sun, and L. H. Xie: Error-constrained LOS path following of a surface vessel with actuator saturation and faults. IEEE Trans. Systems Man Cybernet.: Systems *48* (2018), 1794–1805. DOI:10.1109/TSMC.2017.2717850

Ronghua Lei, School of Mechanical Engineering and Automation, Fuzhou University, Fuzhou 350116 P. R. China.
e-mail: leironh@163.com

Li Chen, School of Mechanical Engineering and Automation, Fuzhou University, Fuzhou 350116. P. R. China.
e-mail: chnle@fzu.edu.cn